

PHYSICOCHEMICAL PRINCIPLES  
OF CREATING MATERIALS AND TECHNOLOGIES

Composite Materials Obtained via Two-Nozzle Electrospinning  
from Polycarbonate and Vinylidene  
Fluoride/Tetrafluoroethylene Copolymer

E. N. Bolbasov<sup>a, \*</sup>, V. M. Buznik<sup>b, \*\*</sup>, K. S. Stankevich<sup>a, \*\*\*</sup>, S. I. Goreninskii<sup>a, \*\*\*\*</sup>,  
Yu. N. Ivanov<sup>c, \*\*\*\*\*</sup>, A. A. Kondrasenko<sup>d, \*\*\*\*\*</sup>, V. I. Gryaznov<sup>e, \*\*\*\*\*</sup>,  
A. N. Matsulev<sup>c, d, \*\*\*\*\*</sup>, and S. I. Tverdokhlebov<sup>a, \*\*\*\*\*</sup>

<sup>a</sup>Tomsk Polytechnic University, Tomsk, 634050 Russia

<sup>b</sup>All-Russian Scientific Research Institute of Aviation Materials, Moscow, 105005 Russia

<sup>c</sup>Kirensky Institute of Physics, Siberian Branch, Russian Academy of Sciences, Krasnoyarsk, 660036 Russia

<sup>d</sup>Institute of Chemistry and Chemical Technology, Siberian Branch, Russian Academy of Sciences, Krasnoyarsk, 660036 Russia

<sup>e</sup>Korotkov Scientific and Production Enterprise Temp, Moscow, 127015 Russia

\*e-mail: Ebolbasov@gmail.com

\*\*e-mail: bouznik@ngs.ru

\*\*\*e-mail: xenia.st88@gmail.com

\*\*\*\*e-mail: semgor93@gmail.com

\*\*\*\*\*e-mail: yuni@iph.krasn.ru

\*\*\*\*\*e-mail: kondrasenko@icct.ru

\*\*\*\*\*e-mail: GryaznovV@ya.ru

\*\*\*\*\*e-mail: matsulev@icct.ru, matsulev@iph.krasn.ru

\*\*\*\*\*e-mail: tverd@tpu.ru

Received April 24, 2017

**Abstract**—Nonwoven composite membranes based on polycarbonate (PC) and vinylidene fluoride/tetrafluoroethylene copolymer were obtained via the two-channel electrospinning method with a common collector. Three groups of materials were studied: the first one was a polymer membrane made of a vinylidene fluoride/tetrafluoroethylene copolymer, the second one was a polymer membrane based on PC, and the third one involved a composite polymer membrane. Scanning electron microscopy studies of morphology of the polymeric membranes showed that a composite material with a variable pore area could be obtained, which allows selection of this parameter depending on the purpose. The resulting composite material and its constituents are studied with nuclear magnetic resonance, IR spectroscopy, X-ray diffraction, and differential scanning calorimetry. There are electrically active crystalline phases in the composite membranes. The obtained nonwoven composite membrane formed is presented as a two-phase system without any chemical interactions between the phases.

**Keywords:** electrospinning, two-nozzle electrospinning, nonwoven composite materials, vinylidene fluoride/tetrafluoroethylene copolymer, polycarbonate, fluoropolymers

**DOI:** 10.1134/S2075113318020065

## INTRODUCTION

Currently, production of semipermeable polymer membranes and study of their structure and properties are the most intensively developing areas of processing of polymer materials. This is to be expected due to large number of their applications in industry [1]. Considering that there is a variety of methods for manufacturing semipermeable polymer membranes, the membranes manufactured via electrospinning (ES) attract special attention [2], because they have high

open porosity, a large free surface area, high strength, etc. Electrospinning allows application of various polymer materials for membranes production and tailoring of their structure and properties in wide range [3]. It should be noted that there is a constant increase in requirements to physicochemical properties together with technical, operational, and economic characteristics of the polymer membranes [4]. One way to meet these demands is production of composite polymer membranes.

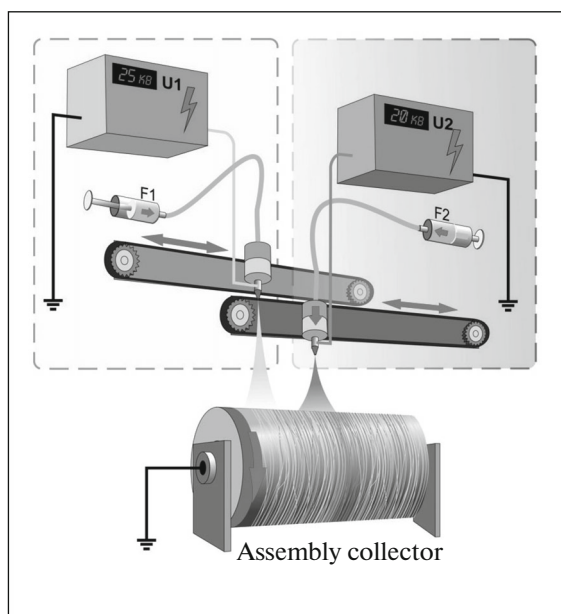


**Fig. 1.** Schematic diagram of a two-nozzle electrospinning setup.

At present, there are two main approaches to obtain composite membranes via ES [5]. The first one is the use of dispersed inorganic reinforcing fillers. The second one is the use of polymer fillers and mixtures of thermodynamically incompatible polymers. In addition, the majority of technological solutions for production of composite polymer membranes by ES method imply use of “single-nozzle” spinning systems [6], which limits the application of this method for their production.

One of the promising methods to produce composite membranes is a two-nozzle electrospinning method (Fig. 1) [7].

Independent control of ES process parameters (type of spinning solution, applied voltage, distance to the collector, flow rate of the spinning solution, etc.) in each channel makes it possible to obtain a wide range of composite membranes from various polymers, including those with incompatible technological parameters (polymer type, solvent, molecular weight, polydispersity etc.). Wide technological possibilities of this method began to attract attention of the scientific community, as evidenced by an increase in the number of publications devoted to this problem in the world.

The general configuration of the systems for two-nozzle ES [8, 9], optimal location of injection nozzles [10], and the influence of spinning process parameters on structure and properties of the composite membranes [11, 12] are being actively studied.

Vinylidene fluoride/tetrafluoroethylene (VDF/TFE) copolymer demonstrates high electrical activity, chemical stability and piezo-, pyro-, and ferroelectric

properties [13, 14]. Chemically resistant polymer membranes formed using two-nozzle electrospinning and obtained from vinylidene fluoride copolymers are used for membrane distillation [15], separation of emulsions [16], and extraction of uranium (U) from seawater [17]. Piezo-, pyro-, and ferroelectric properties of the VDF-TFE copolymer make it possible to produce membranes which change their properties under external electrical, thermal, or mechanical fields.

Polycarbonate (PC) has high impact strength, hardness, and viscosity [18]; it is also a large-tonnage commercially available and inexpensive polymeric material in comparison with VDF-TFE copolymer. Composite membranes made of these polymers can potentially improve their physical and mechanical properties and can decrease their cost, retaining the advantages of fluoropolymers.

The aim of this work was to develop and study the properties of new composite membranes obtained using two-nozzle electrospinning method. This implies production of composites containing fluoropolymers, which possess some properties often not characteristic of hydrocarbon polymers. Two polymeric materials, VDF-TFE and PC, were used to obtain a composite membrane.

## EXPERIMENTAL

The semipermeable polymeric membranes were obtained on a NANON-NF-101 laboratory device (Japan). A common cathode scheme, to which two injection nozzles were connected, was used. The material was collected on a drum collector. The material was produced under the following technological parameters: voltage of 20 kV, flow rate of polymer solutions was 4 mL/h, drum rotation speed was 200 rpm, and distance between needle tip and collector was 70 mm. Two spinning solutions were used: the first was a 7% VDF-TFE copolymer solution (Galopolimer, Russia) in acetone, whereas the second was a 12% PC solution (TRIEX®) in trichloromethane.

Three groups of the materials were obtained in present work: the first one was a polymer membrane made of VDF-TFE copolymer, the second one was a PC polymer membrane, and the third one was a composite polymer membrane.

Morphology of the obtained materials was studied by scanning electron microscopy (SEM) on a NeoScope JCM-6000 microscope (JEOL, Japan) equipped with a secondary electron detector in a low vacuum mode. For this purpose, a thin layer of gold was applied on the surface in an SC7640 magnetron sputtering system (Quorum Technologies, England). Fiber diameter was determined from images of five different sections of the materials samples Image J 1.38 software (National Institutes of Health, United States) from not less than 50 measurements.

Chemical structure of the samples was studied by means of attenuated total reflection infrared spectroscopy (ATR IR) using Tensor 27 spectrometer (Bruker) equipped with a PIKE MIRacle (Bruker) console on a ZnSe crystal. The studies were carried out within the spectral range from 500 to 2000  $\text{cm}^{-1}$  with a resolution of 4  $\text{cm}^{-1}$ .

Crystal structure of the samples was studied using X-ray diffraction on a XRD 6000 diffractometer (Shimadzu) with wavelength of 1.54056 Å at the following parameters: accelerating voltage – 30 kV, beam current – 30 mA, scanning range –  $10^{\circ}$ – $30^{\circ}$ , scanning step –  $0.02^{\circ}$ , and acquisition time was 1 s.

Thermal properties of the samples were studied using differential scanning calorimetry (DSC) on a DSC 204F1 Phoenix (Netzsch) within the temperature range of 70– $230^{\circ}\text{C}$  and sample heating rate of  $10^{\circ}\text{C}/\text{min}$ . The sample weight was  $3.5 \pm 0.1$  mg.

$^1\text{H}$ ,  $^{13}\text{C}$ , and  $^{19}\text{F}$  NMR spectra of the membranes were recorded using Avance 300 and Avance 600 pulsed NMR spectrometers within the temperature range from 150 to 380 K.  $^1\text{H}$  and  $^{19}\text{F}$  NMR spectra were acquired by method of Fourier spectroscopy on the Avance 300 spectrometer, whereas  $^{13}\text{C}$  spectra were obtained via the proton cross-polarization method. The  $^1\text{H}$  and  $^{13}\text{C}$  NMR spectra were obtained on the Avance 600 spectrometer upon magical angle spinning (MAS).

## RESULTS AND DISCUSSION

Figure 2 shows SEM-images of the polymer membranes from three groups at different magnifications.

Polymer membrane made of VDF-TFE copolymer was presented by randomly entangled fibers with an average diameter of  $0.7 \pm 0.2$   $\mu\text{m}$ . There is a high packing density of the fibers in the membrane (Fig. 2a).

Membrane obtained from PC solution consisted from fibers with an average diameter of  $6.7 \pm 2.2$   $\mu\text{m}$ . Cylindrical microfibers with an average diameter of  $1.2 \pm 0.4$   $\mu\text{m}$  fill the space between macrofibers. PC membranes demonstrated lower packing density of fibers and, as a result, greater porosity compared to VDF-TFE copolymer. Pore areas in the VDF-TFE and PC membranes were  $49 \pm 16$  and  $788 \pm 373$   $\mu\text{m}^2$ , respectively (Fig. 2b).

There are two types of fibers in the structure of the composite membrane (Fig. 2c). The first type involves fibers with an average diameter of  $6.3 \pm 1.6$   $\mu\text{m}$ , whereas the second type is presented by fibers with an average diameter of  $0.8 \pm 0.6$   $\mu\text{m}$ , which fill the space between fibers of the first type. Average pore area in the resulting composite membrane was  $247 \pm 130$   $\mu\text{m}^2$ . The corresponding parameters of the membranes obtained from individual polymers indicate that the fibers of the first type are polycarbonate, whereas those of the second type are fluoropolymer.

It is known that direct observation of the ferroelectric properties ( $E$ – $D$  hysteresis loops) for the VDF-TFE copolymer is possible in electric fields with a strength of more than 40 MV/m [19], which requires production of homogeneous and defect-free samples that exclude electric breakdown [20, 21]. Obtained materials contain a significant amount of pores, which dramatically decreases their electrical strength. Polymorphic conformations and crystal structures characteristic of paraelectric and ferroelectric phases in the VDF-TFE copolymer allow them to be detected with IR spectroscopy, X-ray diffraction, and DSC [22].

Figure 3 shows ATR IR spectra of the samples.

The IR spectrum of the membrane obtained from VDF-TFE copolymer solution contains several main absorption bands. Those at frequencies of 884, 1398, 1327, and 1430  $\text{cm}^{-1}$  are characteristic of the electrically active TTT conformation [23, 24], the band at 821  $\text{cm}^{-1}$  is typical of the electrically active  $\text{T}_3\text{GT}_3\text{G}^-$  conformation [25], and the band at 620  $\text{cm}^{-1}$  corresponds to the paraelectric  $\text{TGTG}^-$  one [26]. The absorption bands corresponding to electrically active conformations demonstrate that the membrane can possess piezo-, pyro-, and ferroelectric properties [19, 27].

Spectrum of the membrane formed from PC fibers contains characteristic absorption bands. The band at 763  $\text{cm}^{-1}$  is assigned to deformation vibrations of a C–H group in the aromatic ring and the band at 1190  $\text{cm}^{-1}$  is typical of C–O deformation vibrations in the aromatic ring. The band at 1504  $\text{cm}^{-1}$  is ascribed to the vibrations of a C–H group in the aromatic ring [28], whereas the bands at 1600 and 1773  $\text{cm}^{-1}$  are typical of valence vibrations of the C=O group [29, 30].

Spectrum of the composite membrane contains all bands characteristic of individual components. Moreover, there is an effect of addition of spectral density for overlapping bands of individual components at 884 and 1158  $\text{cm}^{-1}$ . The fact that there are no shifts of the absorption bands and that there are new bands indicates that there are no chemical interactions between the components of the composite membrane. The bands at 1398 and 884  $\text{cm}^{-1}$  indicate that the membrane formed possesses piezo-, pyro-, and ferroelectric properties.

Figure 4 shows X-ray diffractograms of the studied polymer membranes.

There are several reflexes on the X-ray diffraction pattern of the VDF-TFE polymer membrane. A halo in the  $16^{\circ}$ – $18^{\circ}$  region corresponds to a paraelectric  $\alpha$  phase, whereas a small and completely distinguishable reflex at  $18.6^{\circ}$  is assigned to the reflection from the (020) plane of the electrically active  $\gamma$  phase. In addition, the most intensive reflex at  $19.3^{\circ}$  is characteristic for reflection from the (110) and (200) planes of the electrically active  $\beta$  phase [24, 28]. An intense reflex at  $19.3^{\circ}$  indicates that macromolecules in the membrane fibers based on VDF-TFE copolymer form

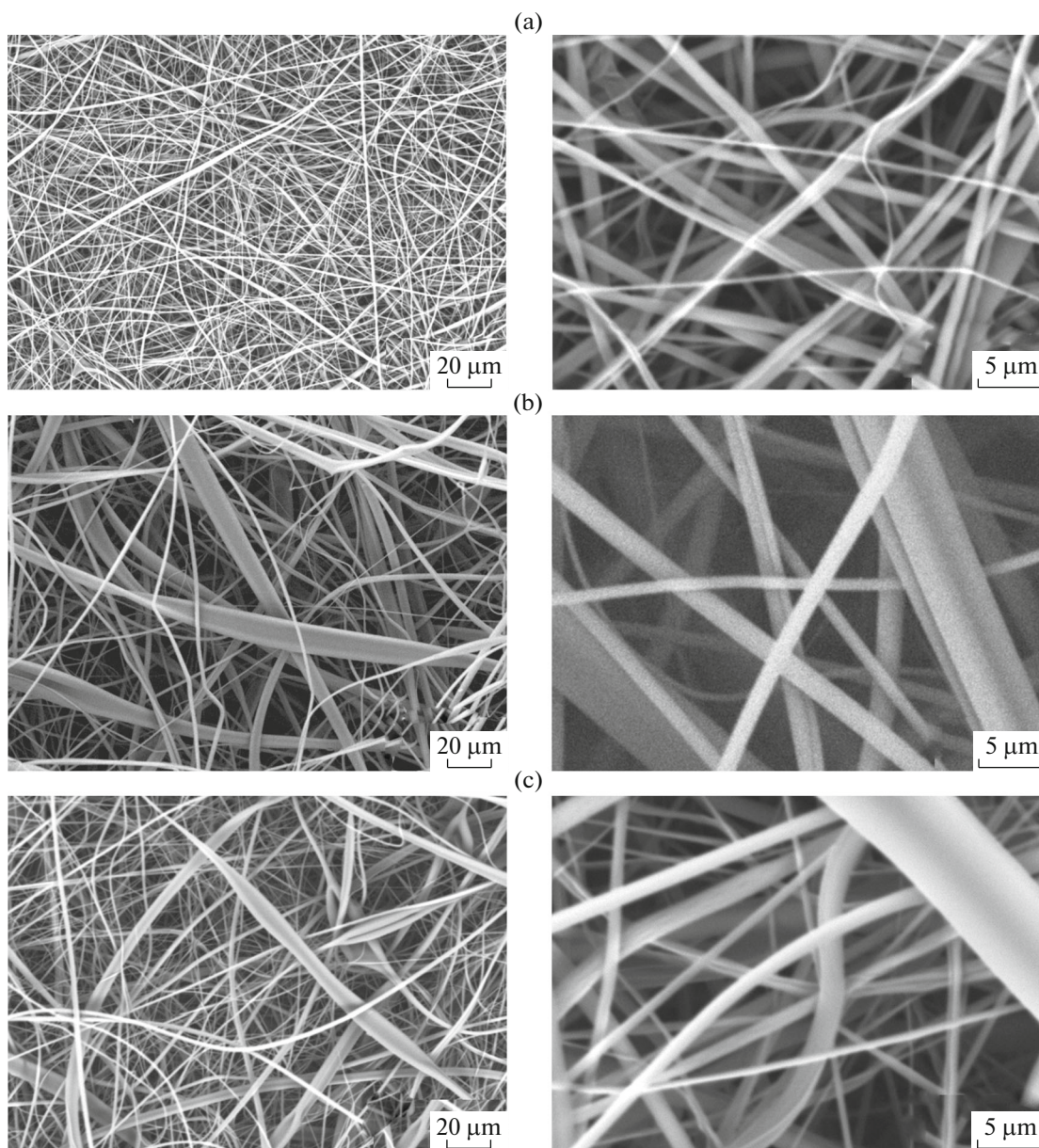


**Fig. 2.** SEM images of the polymer membranes obtained via electrospinning from (a) VDF-TFE copolymer, (b) PC, and (c) VDF-TFE/PC composite membrane.

crystal structures possessing piezo-, pyro-, and ferroelectric properties. IR studies confirm these findings.

There is a broad halo at  $12^{\circ}$ – $22^{\circ}$  on the X-ray diffraction pattern of the membrane obtained from PC solution. This indicates that the macromolecules forming the fibers in the membrane are predominantly in the amorphous phase.

The differences observed in the crystal structure of the samples are probably due to two main reasons: a significant difference in flexibility and interaction between dipole moments of the macromolecules and external electric field. Macromolecules of the VDF-TFE copolymer, which have a significant dipole

moment and high flexibility, exposed to high intensity external electric field together with a spinning solution form structures being more ordered topologically. Intense evaporation of the solvent from the stream of spinning solution limits the mobility of the macromolecules and “freezes” the ordered structure to form crystallites.

PC does not possess a high dipole moment or flexibility of macromolecules, which makes it difficult for them to be located in the stream of spinning solution exposed to an external electric field. Intense evaporation of the solvent leads to amorphous structures, “freezing” the system with high entropy.

A reflex at  $19.3^\circ$  was observed on the X-ray diffraction pattern of the nonwoven composite material against the background of halo at  $12^\circ$ – $22^\circ$ . The fact that there is no shift of this reflex and no significant differences in the FWHM parameter were observed for the nonwoven composite and VDF-TFE copolymer membranes indicates that the electrically active  $\beta$  phase is identical in both types of membranes. Thus, there are no chemical interactions between the components forming the polymer composite.

Figure 5 shows thermograms of the samples studied. VDF-TFE membranes had an intense endothermic effect at  $144^\circ\text{C}$  described earlier [32, 33]. This is due to overlap of an endothermic effect caused by the Curie transition and endothermic melting effect of the crystalline phases in VDF-TFE copolymer, which has significant residual polarization after the action of the external electric field.

Thermogram of the PC nonwoven material shows an endothermic transition at  $146^\circ\text{C}$ , which is attributed to a transition from the glassy state to the molten one [34]. Moreover, it should be noted that the endothermic anomalies observed on thermograms of PC and VDF-TFE copolymer have a different form, which is probably due to the amorphous structure of PC. The fact that there are no effects due to first-order transitions on the thermogram confirms that PC macromolecules in the nonwoven material do not form crystalline structures, which is in agreement with the results previously obtained [29].

Thermogram of the nonwoven composite material contains an intense endothermic effect at  $146^\circ\text{C}$ , which is due to superposition of melting effects of components in the composite material. The fact that there are no other thermal effects on the thermogram indicates that there are no strong chemical interactions between components in the composite material; X-ray diffraction and IR spectroscopy data confirm this fact.

$^{19}\text{F}$  NMR spectra of the VDF-TFE membranes and VDF-TFE/PC composites were acquired via Fourier pulse spectroscopy in the range of 150–380 K. Figure 6 shows the temperature dependence of fluorine NMR spectra for the VDF-TFE copolymer sample.

$^{19}\text{F}$  NMR line is greatly broadened almost throughout the temperature range, which is due to dipole–dipole interaction between magnetic moments of the neighboring fluorine and hydrogen nuclei (F–F and F–H) and due to anisotropy of the  $^{19}\text{F}$  chemical shift tensors. However, at a temperature of 380 K (near the melting point of the sample), the dipole interactions and anisotropic part of the chemical shift tensors are averaged owing to rapid motion of the fluorine and proton atoms. Position of the  $^{19}\text{F}$  NMR lines at high temperature, therefore, is determined only by an isotropic chemical shift as in the spectra of liquid samples. High-resolution  $^{19}\text{F}$  NMR spectrum of the VDF-TFE copolymer (in acetone- $\text{D}_6$ ) was studied, and it

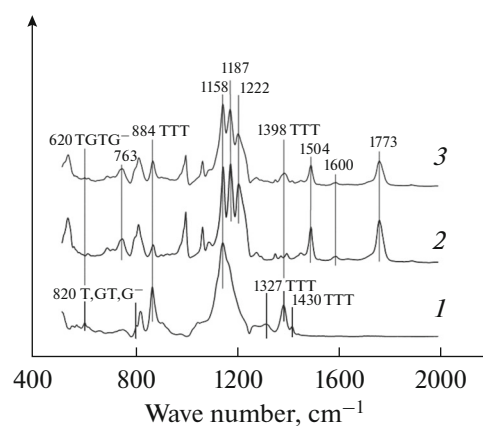


Fig. 3. IR spectra of the samples: (1) VDF-TFE copolymer, (2) PC, and (3) VDF-TFE/PC composite membrane.

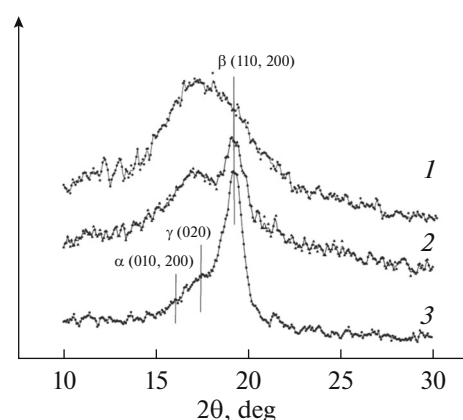


Fig. 4. XRD patterns of the polymer membranes: (1) PC, (2) VDF-TFE/PC composite membrane, and (3) VDF-TFE copolymer.

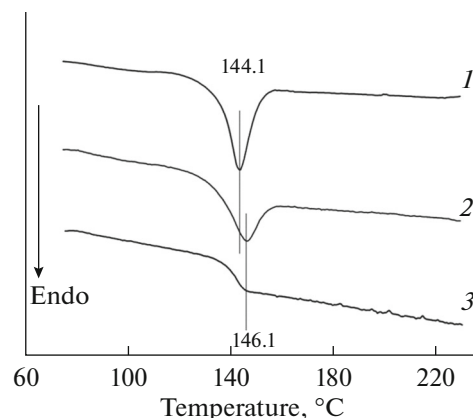
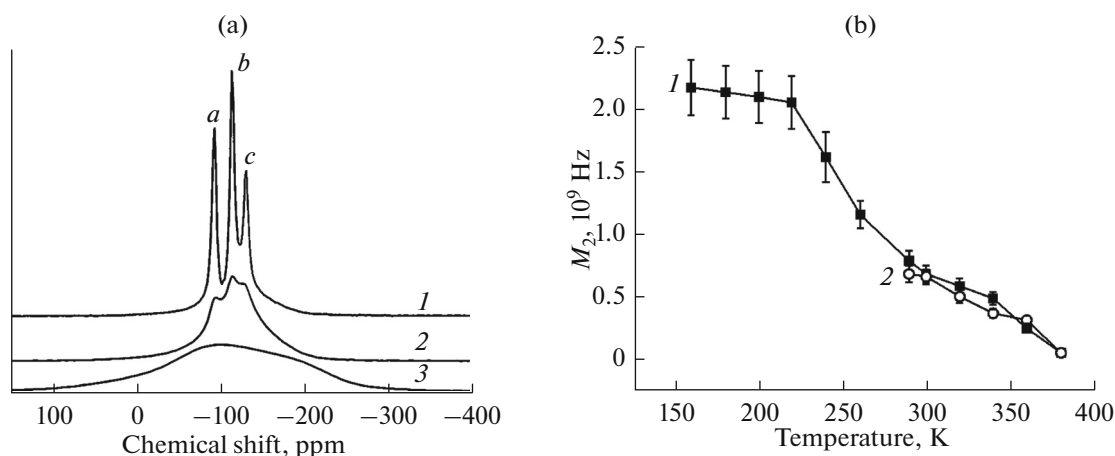


Fig. 5. DSC curves of the samples: (1) VDF-TFE copolymer, (2) VDF-TFE/PC composite membrane, and (3) PC.

was found that it contains three groups of lines [35]. Isotropic part of the chemical shift depends on the nearest environment of a resonant nucleus. There are three different possible environments for the fluorine



**Fig. 6.** Temperature dependence for (a)  $^{19}\text{F}$  NMR spectra of VDF-TFE, where chemical shifts are scaled relative to trichlorofluoromethane ( $\text{CCl}_3\text{F}$ ), acquired at (1) 380, (2) 360, and (3) 160 K and (b)  $^{19}\text{F}$  NMR spectra of the second moments in (1) VDF-TFE and (2) VDF-TFE/PC composite.

atom in the  $\text{CF}_2$  difluoromethylene unit of the copolymer: (a)  $-\text{CH}_2-\text{CF}_2-\text{CH}_2-$ , (b)  $-\text{CH}_2-\text{CF}_2-\text{CF}_2-$ , and (c)  $-\text{CF}_2-\text{CF}_2-\text{CF}_2-$ . Each such group in the spectra acquired for any liquids provides several lines owing to influence of distant neighbors, which are not distinguishable in the spectrum of a solid substance. Positions of the *a*, *b*, and *c* peaks in the  $^{19}\text{F}$  spectrum (Fig. 6a), however, precisely coincide with the centers of gravity of the corresponding line groups in the high-resolution spectra [35, 36] ( $\delta_{\text{F}}(a) = -92 \pm 2$  ppm,  $\delta_{\text{F}}(b) = -113 \pm 2$  ppm, and  $\delta_{\text{F}}(c) = -125 \pm 2$  ppm). The integral intensity of each component in the  $^{19}\text{F}$  spectrum (Fig. 6a) is proportional to the number of  $\text{CF}_2$  difluoromethylene units in corresponding positions (*a*, *b*, and *c*) in the VDF-TFE copolymer. This allows determination of relative molar fractions of vinylidene fluoride and tetrafluoroethylene in the VDF-TFE copolymer according to the formula [36]

$$\text{VDF} [\text{mol} \%] = \frac{200(2a + b)}{4a + 3b + 2c},$$

where *a*, *b*, and *c* are the corresponding integral intensities of the  $^{19}\text{F}$  NMR signals. Calculations show that our copolymer contains  $70 \pm 5$  mol % of VDF.

$^{19}\text{F}$  spectra of the VDF-TFE/PC composite material were studied in the range of 290–390 K and were acquired under the same conditions as for the VDF-TFE copolymer. Figure 7 shows the  $^{19}\text{F}$  NMR spectra of the VDF-TFE/PC composite material and VDF-TFE copolymer at 380 K.

Figure 7 shows that the spectra differ only in the presence of a broad component of the VDF-TFE copolymer, which indicates the presence of inactive positions of fluorine atoms, apparently belonging to the crystalline phase of VDF-TFE. Nevertheless, we may assume that VDF-TFE copolymer chains in the VDF-TFE/PC composite do not undergo changes in comparison with the original polymer; in other words, the composite material is presented as a two-phase VDF-TFE/PC system. Almost complete temperature dependences of change in the second moment of the  $^{19}\text{F}$  NMR spectral lines of the VDF-TFE and VDF-TFE/PC composite (Fig. 6b) confirm this finding (the second moment is a quantitative characteristic of spectral line width, which is due to internal interactions in the substance). The second moments at low temperatures coincide with experimental accuracy, whereas small differences shown in Figure 6b appear only at temperatures above room temperature. The electronic structure and topology of fluorine atoms in the  $\text{CF}_2$  groups, as well as mobility of fluorine atoms in both samples, therefore, are identical. Our analysis of integral intensities in the  $^{19}\text{F}$  NMR spectra shown in Fig. 7, taking into account the weight of the corresponding samples, indicates that the amount of VDF-TFE copolymer in the VDF-TFE/PC composite is  $35 \pm 5\%$ .

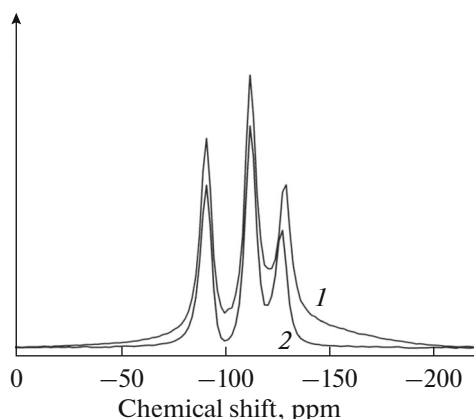


**Fig. 7.**  $^{19}\text{F}$  NMR spectra for (1) VDF-TFE copolymer and (2) VDF-TFE/PC composite at 380 K.

## CONCLUSIONS

Nonwoven composite material was obtained from polycarbonate and vinylidene fluoride/tetrafluoroethylene copolymer via two-nozzle electrospinning with common collector. The structure of the composite material and its components was studied.

Composite structure of the obtained membrane allows tailoring of the pores area depending on requirements to the material.

Infrared spectroscopy, X-ray diffraction, and differential scanning calorimetry data showed the presence of electrically active crystalline phases in the composite membranes.

NMR, infrared spectroscopy, and X-ray diffraction data indicated that the composite nonwoven membrane is a two-phase system without chemical interactions between phases.

## ACKNOWLEDGMENTS

The membranes were prepared and studied by means of scanning electron microscopy and X-ray diffraction at the Tomsk National Research Polytechnic University under financial support of the Russian Science Foundation (project no. 16-13-10239). NMR studies were financially supported by the Russian Foundation for Basic Research (project no. 14-29-10178 ofi\_m) and performed at the Kirensky Institute of Physics, Siberian Branch, Russian Academy of Sciences.

## REFERENCES

- Gugliuzza, A. and Drioli, E., A review on membrane engineering for innovation in wearable fabrics and protective textiles, *J. Membr. Sci.*, 2013, vol. 446, pp. 350–375. doi 10.1016/j.memsci.2013.07.014
- Filatov, Y., Budyka, A., and Kirichenko, V., *Electrospinning of Micro- and Nanofibers: Fundamentals in Separation and Filtration Processes*, New York: Begell House, 2007.
- Reneker, D.H. and Chun, I., Nanometre diameter fibers of polymer, produced by electrospinning, *Nanotechnology*, 1996, vol. 7, pp. 216–223. doi 10.1088/0957-4484/7/3/009
- Kablov, E.N., Materials and chemical technologies for aircraft engineering, *Herald Russ. Acad. Sci.*, 2012, vol. 82, no. 3, pp. 158–167. doi 10.1134/S1019331612030069
- Huang, Z.-M., Zhang, Y.-Z., Kotaki, M., and Ramakrishna, S., A review on polymer nanofibers by electrospinning and their applications in nanocomposites, *Compos. Sci. Technol.*, 2003, vol. 63, pp. 2223–2253. doi 10.1016/S0266-3538(03)00178-7
- Teo, W.E. and Ramakrishna, S., A review on electrospinning design and nanofiber assemblies, *Nanotechnology*, 2006, vol. 17, pp. R89–R106. doi 10.1088/0957-4484/17/14/R01
- Zhang, C., Li, Y., Wang, W., Zhan, N., Xiao, N., Wang, S., Li, Y., and Yang, Q., A novel two-nozzle electrospinning process for preparing microfiber reinforced pH sensitive nano-membrane with enhanced mechanical property, *Eur. Polym. J.*, 2011, vol. 47, pp. 2228–2233. doi 10.1016/j.eurpolymj.2011.09.015
- Hajiani, F., Jeddi, A.A.A., and Gharehaghaji, A.A., An investigation on the effects of twist on geometry of the electrospinning triangle and polyamide 66 nanofiber yarn strength, *Fibers Polym.*, 2012, vol. 13, pp. 244–252. doi 10.1007/s12221-012-0244-3
- Dabirian, F. and Hosseini, S.A., Novel method for nanofiber yarn production using two differently charged nozzles, *Fibres Text. East. Eur.*, 2009, vol. 74, pp. 45–47.
- Park, C.H., Pant, H.R., and Kim, C.S., Novel robot-assisted angled multi-nozzle electrospinning set-up: computer simulation with experimental observation of electric field and fiber morphology, *Text. Res. J.*, 2014, vol. 84, pp. 1044–1058. doi 10.1177/0040517513517961
- Tijing, L.D., Choi, W., Jiang, Z., Amarjargal, A., Park, C.H., Pant, H.R., Im, I.T., and Kim, C.S., Two-nozzle electrospinning of (MWNT/PU)/PU nanofibrous composite mat with improved mechanical and thermal properties, *Curr. Appl. Phys.*, 2013, vol. 13, pp. 1247–1255. doi 10.1016/j.cap.2013.03.023
- Zhan, N., Li, Y., Zhang, C., Song, Y., Wang, H., Sun, L., Yang, Q., and Hong, X., A novel multinozzle electrospinning process for preparing superhydrophobic PS films with controllable bead-on-string/microfiber morphology, *J. Colloid Interface Sci.*, 2010, vol. 345, pp. 491–495. doi 10.1016/j.jcis.2010.01.051
- Kochervinskii, V.V., The structure and properties of block poly(vinylidene fluoride) and systems based on it, *Rus. Chem. Rev.*, 1996, vol. 65, no. 10, pp. 865–913. doi 10.1070/RC1996v065n10ABEH000328
- Furukawa, T., Ferroelectric properties of vinylidene fluoride copolymers, *Phase Trans.*, 1989, vol. 18, pp. 143–211. doi 10.1080/01411598908206863
- Lee, E.-J., An, A.K., Hadi, P., Lee, S., Woo, Y.C., and Shon, H.K., Advanced multi-nozzle electrospun functionalized titanium dioxide/polyvinylidene fluoride-cohexafluoropropylene (TiO<sub>2</sub>/PVDF-HFP) composite membranes for direct contact membrane distillation, *J. Membr. Sci.*, 2017, vol. 524, pp. 712–720. doi 10.1016/j.memsci.2016.11.069
- Wang, X., Yu, J., Sun, G., and Ding, B., Electrospun nanofibrous materials: a versatile medium for effective oil/water separation, *Mater. Today*, 2016, vol. 19, pp. 403–414. doi 10.1016/j.mattod.2015.11.010
- Xie, S., Liu, X., Zhang, B., Ma, H., Ling, C., Yu, M., Li, L., and Li, J., Electrospun nanofibrous adsorbents for uranium extraction from seawater, *J. Mater. Chem. A*, 2015, vol. 3, pp. 2552–2558. doi 10.1039/C4TA06120A
- Greco, R. and Sorrentino, A., Polycarbonate/ABS blends: A literature review, *Adv. Polym. Technol.*, 1994, vol. 13, pp. 249–258. doi 10.1002/adv.1994.060130401
- Kochervinskii, V.V., Specifics of structural transformations in poly(vinylidene fluoride)-based ferroelectric polymers in high electric fields, *Polym. Sci., Ser. C*, 2008, vol. 50, pp. 93–121. doi 10.1134/S1811238208010062
- Hicks, J.C., Jones, T.E., and Logan, J.C., Ferroelectric properties of poly(vinylidene fluoride-tetrafluoroethylene), *J. Appl. Phys.*, 1978, vol. 49, p. 6092. doi 10.1063/1.324528
- Tasaka, S. and Miyata, S., Effects of crystal structure on piezoelectric and ferroelectric properties of

- copoly(vinylidene fluoride-tetrafluoroethylene), *J. Appl. Phys.*, 1985, vol. 57, p. 906. doi 10.1063/1.334691
22. Martins, P., Lopes, A.C., and Lanceros-Mendez, S., Electroactive phases of poly(vinylidene fluoride): determination, processing and applications, *Prog. Polym. Sci.*, 2014, vol. 39, pp. 683–706. doi 10.1016/j.progpolymsci.2013.07.006
  23. Tashiro, K., Abe, Y., and Kobayashi, M., Computer simulation of structure and ferroelectric phase transition of vinylidene fluoride copolymers (1) vdf content dependence of the crystal structure, *Ferroelectrics*, 1995, vol. 171, pp. 281–297. doi 10.1080/00150199508018440
  24. Ermolinskaya, T.M., Fen'ko, L.A., and Bil'dyukevich, A.V., Effect of a solvent on the solution behavior of Teflon-42 and the structure of related films, *Polym. Sci., Ser. A*, 2008, vol. 50, pp. 1065–1070. doi 10.1134/S0965545X08100076
  25. Tashiro, K., Kaito, H., and Kobayashi, M., Structural changes in ferroelectric phase transitions of vinylidene fluoride-tetrafluoroethylene copolymers: 1. Vinylidene fluoride content dependence of the transition behavior, *Polymer*, 1992, vol. 33, pp. 2915–2928. doi 10.1016/0032-3861(92)90077-A
  26. Bormashenko, Y., Pogreb, R., Stanevsky, O., and Bormashenko, E., Vibrational spectrum of PVDF and its interpretation, *Polym. Test.*, 2004, vol. 23, pp. 791–796. doi 10.1016/j.polymertesting.2004.04.001
  27. Kochervinskii, V.V., Kiselev, D.A., Malinkovich, M.D., Pavlov, A.S., and Malyshkina, I.A., Local piezoelectric response, structural and dynamic properties of ferroelectric copolymers of vinylidene fluoride-tetrafluoroethylene, *Colloid Polym. Sci.*, 2014. doi 10.1007/s00396-014-3435-1
  28. Delpech, M.C., Coutinho, F.M., and Habibe, M.E.S., Bisphenol A-based polycarbonates: Characterization of commercial samples, *Polym. Test.*, 2002, vol. 21, pp. 155–161. doi 10.1016/S0142-9418(01)00063-0
  29. Liao, C.-C., Wang, C.-C., Shih, K.-C., and Chen, C.-Y., Electrospinning fabrication of partially crystalline bisphenol A polycarbonate nanofibers: Effects on conformation, crystallinity, and mechanical properties, *Eur. Polym. J.*, 2011, vol. 47, pp. 911–924. doi 10.1016/j.eurpolymj.2011.01.006
  30. Heymans, N. and van Rossum, S., FTIR investigation of structural modifications during low-temperature ageing of polycarbonate, *J. Mater. Sci.*, 2002, vol. 37, pp. 4273–4277. doi 10.1023/A:1020636115507
  31. Kochervinskii, V.V., Glukhov, V.A., Sokolov, V.G., Romadin, V.F., Murasheva, Y.M., Ovchinnikov, Y.K., Trofimov, N.A., and Lokshin, B.V., Microstructure and crystallization of isotropic films made of vinylidene fluoride-tetrafluoro-ethylene copolymer, *Polym. Sci. U.S.S.R.*, 1988, vol. 30, no. 9, pp. 2100–2108. doi 10.1016/0032-3950(88)90067-6
  32. Murata, Y., Curie transition in poled and unpoled copolymer of vinylidene fluoride and tetrafluoroethylene, *Polym. J.*, 1987, vol. 19, pp. 337–346. doi 10.1295/polymj.19.337
  33. Murata, Y. and Koizumi, N., Ferroelectric behavior in vinylidene fluoride-tetrafluoroethylene copolymers, *Ferroelectrics*, 1989, vol. 92, pp. 47–54. doi 10.1080/00150198908211305
  34. Hu, X. and Lesser, A.J., Enhanced crystallization of bisphenol-A polycarbonate by nano-scale clays in the presence of supercritical carbon dioxide, *Polymer*, 2004, vol. 45, pp. 2333–2340. doi 10.1016/j.polymer.2003.12.079
  35. Li, L., Twum, E.B., Li, X., McCord, E.F., Fox, P.A., Lyons, D.F., and Rinaldi, P.L., 2D-NMR characterization of sequence distributions in the backbone of poly(vinylidene fluoride-co-tetrafluoroethylene), *Macromolecules*, 2012, vol. 45, pp. 9682–9696. doi 10.1021/ma3020307
  36. Cais, R.E. and Kometani, J.M., Structural studies of vinylidene fluoride-tetrafluoroethylene copolymers by nuclear magnetic resonance spectroscopy, *Anal. Chim. Acta*, 1986, vol. 189, pp. 101–116. doi 10.1016/S0003-2670(00)83717-4

Translated by A. Tulyabaev